European Journal of Radiology Open 7 (2020) 100294

Contents lists available at ScienceDirect

European Journal of Radiology Open

journal homepage: www.elsevier.com/locate/ejro

Chest CT imaging features of COVID-19 pneumonia: First radiological insights from Porto, Portugal

A. Carvalho [a,*], R. Cunha [a], B.A. Lima [b], J.M. Pereira [a], A.J. Madureira [a]

[a] Serviço de Radiologia, Centro Hospitalar Universitário de São João, EPE, Portugal
[b] Oficina de Bioestatística, Portugal

HIGHLIGHTS

- The most common imaging findings of COVID-19 in our patient group were multilobar ground-glass opacities and parenchymal consolidation.
- Older age, opacities with diffuse distribution in the axial plane and a higher CT severity index were associated with worse short-term prognosis.
- The presence of rounded opacities or patterns resembling organizing pneumonia were associated with favorable short-term prognosis.

ARTICLE INFO

Keywords:
COVID-19
SARS-CoV-2
Computed tomography
Chest

ABSTRACT

Introduction: The outbreak of a highly infectious respiratory disease – COVID-19 - has spread globally and a novel type of coronavirus (SARS-CoV-2) was identified as its cause. Chest CT findings have been described as an aid for COVID-19 diagnosis and management. We aimed to describe the CT imaging characteristics in a group of COVID-19 patients while we also intended to assess if any of these radiological features were associated with short-term prognosis.

Materials and methods: CT examinations from 164 consecutive patients with at least one positive RT-PCR nucleic acid assay for SARS-CoV-2 were retrospectively analyzed. Numerous CT imaging features were recorded independently by two radiologists. Patients were grouped according to their status 14 days after the initial CT scan in either discharged/hospitalized in a non-ICU ward (favorable prognosis group) versus deceased/admitted to an intensive care unit (unfavorable prognosis group).

Results: Ground-glass opacities (89.0 %) and consolidations (73.2 %) with multilobar involvement were the predominant imaging findings, while a nodular pattern (3.7 %) and cavitation (1.2 %) were uncommon. Mean age was higher in the mortality/ICU group. Ground-glass opacities and consolidations were dominant in both groups, but distribution pattern of abnormalities was different, being more often diffuse in the mortality/ICU group. Linear opacities and opacities that were rounded in shape were more frequently observed in the favorable prognosis group. CT severity index was significantly higher in the mortality/ICU group. For assessing unfavorable prognosis, the best cut-off for CT severity index was 24 (sensitivity 78 %; specificity 59 %). Interobserver agreement for all CT findings was excellent.

Conclusion: COVID-19 pneumonia in Porto, Portugal, manifests as multilobar ground-glass opacities and consolidations. Older age, diffuse distribution and increasing CT severity index are associated with worse short-term prognosis while linear opacities resembling organizing pneumonia and rounded opacities herald a more favorable prognosis.

1. Introduction

The outbreak of coronavirus disease 2019 (COVID-19), a highly infectious respiratory disease first reported in Wuhan, Hubei province, China in December 2019, has now spread globally infecting more than 26 million people in the whole world and caused more than 864,000

* Corresponding author at: Centro Hospitalar Universitário de São João, EPE, Serviço de Radiologia, Alameda Prof. Hernâni Monteiro, 4200-319, Porto, Portugal.
E-mail addresses: andre.silva.carvalho@chsj.min-saude.pt (A. Carvalho), rui.cunha@chsj.min-saude.pt (R. Cunha), balima78@gmail.com (B.A. Lima), jose.jesus@chsj.min-saude.pt (J.M. Pereira), antonio.madureira@chsj.min-saude.pt (A.J. Madureira).

https://doi.org/10.1016/j.ejro.2020.100294
Received 20 October 2020; Received in revised form 13 November 2020; Accepted 16 November 2020
Available online 28 November 2020

fatalities as of 4 September 2020 [1,2]. A new type of coronavirus with over 70 % genetic similarity to SARS-CoV was identified as the culprit and named SARS-CoV-2 by the World Health Organization (WHO) [3–5]. In Portugal the first case was confirmed on March 2, 2020. Since then, more than 59,000 cases have been confirmed, with approximately 40 % being reported in the Northern region of the country [6]. Diagnosis of COVID-19 is mainly based on clinical and epidemiological criteria, with reverse transcription polymerase chain reaction (RT-PCR) being considered the gold-standard for diagnosis [7]. It is well established that chest CT findings are important in the diagnosis and management of respiratory diseases and numerous recent studies addressed the most common radiological findings of COVID-19 infection [8–19]. These encompass bilateral, multilobar ground-glass opacities with or without consolidation or interlobular and intralobular septal thickening (the so-called crazy-paving pattern) and features of organizing pneumonia (band-like opacities, perilobular opacities and reverse halo sign). The main purpose of this study was to review and describe the chest CT findings in a group of patients with RT-PCR confirmed SARS-CoV-2 infection. We also aimed to assess the relationship, if any, between imaging findings at presentation and short-term prognosis of these patients.

2. Materials and methods

2.1. Patients

This retrospective study was approved by the Institutional Review Boards of our Hospital and written informed consent was waived by the ethical committee.

Between March 3 and April 19, 2020, 186 CT examinations from 164 consecutive patients were retrospectively analyzed. All patients had at least one positive result by RT-PCR nucleic acid assay for SARS-CoV-2 in respiratory secretions obtained either by naso/oropharyngeal swab, coughing or endotracheal aspirate. For the assessment of short-term prognosis, patients were grouped according to their status at 14 days after the initial CT scan in either discharged/hospitalized in a non-ICU ward (favorable prognosis group) versus deceased/admitted to an intensive care unit (unfavorable prognosis group).

2.2. CT acquisition and interpretation

CT scans were obtained with patients in supine position at full end-inspiration, using one of the following two scanners: SOMATOM go. Up or SOMATOM go.Now (Siemens Healthineers, Germany). One-hundred sixty-eight (90.3 %) examinations were performed without use of contrast media and 18 (9.7 %) examinations were done with intravenous contrast use. Images were reconstructed with slice thickness of 3 mm (with 3 mm reconstruction intervals) and 1 mm (with 10 mm reconstruction intervals). CT examinations were archived in picture archiving and communication systems (PACS) and were analyzed independently by two radiologists (A.C. and R. C., with 6 and 18 years of experience in chest CT interpretation, respectively). Evaluators read CT features using axial or multiplanar reconstructed images either in lung and mediastinal window settings. Each scan was evaluated for: (a) presence of ground-glass opacities, (b) presence of consolidation, (c) number of involved pulmonary lobes, (d) presence of predominantly nodular pattern, (e) presence of crazy-paving pattern, (f) presence of cavitation, (g) presence of pleural effusion, (h) presence of mediastinal or hilar lymphadenopathy, defined as lymph-node short-axis $\geq$ 10 mm, (i) presence of underlying lung disease, such as emphysema, fibrosing lung disease or bronchiectasis, (j) presence of linear opacities resembling patterns of organizing pneumonia, such as band-like opacities, reverse halo sign and perilobular opacities, (k) airspace opacification distribution pattern and (l) presence of the halo sign. All radiological findings were assessed as defined by the glossary of terms from the Fleischner Society [20]. The number of involved pulmonary lobes ranged from 1 to 5 with the lingula counting as part of the left upper lobe. Opacification distribution pattern was defined as peripheral if it involved the outer-third of the lung on axial slices, as central if involved mainly the two inner-thirds or as mixed if no predominance was observed. We also applied a "CT severity index" as described by Feng and colleagues [21]. Briefly, we divided the lung in 6 zones: upper, mid and lower zones (both right and left) using the carina and right inferior pulmonary vein as anatomical landmarks. A CT score of 2 was applied for ground-glass opacities and of 3 for consolidation. Involvement of each lung zone was then categorized according to the extent of disease: 0 as normal, 1 as $<$ 25 % involvement, 2 as 25–50 % involvement, 3 as 50–75 % involvement and 4 as $>$75 % involvement. The four-point scale of the lung parenchyma disease extension was multiplied by the CT score and points from all zones were summed for a final total score which ranged from 0 to 72. Discrepancies in radiological assessment were resolved by consensus.

2.3. Statistical analysis

Categorical variables are presented as numbers (and percentages), while continuous variables are presented as means (and standard deviations). In the univariate analysis, Chi-square test was performed to assess differences between frequencies and *t*-test was used to compare mean values between patients with favorable and unfavorable prognosis. A multivariate logistic regression model was also performed. Variables in the final model were selected by a stepwise method both backwards and forwards. Those final variables in the logistic regression model are independently associated with the prognosis at 14 days. The Hosmer–Lemeshow goodness-of-fit test was used to evaluate the overall fit of the final model. Interobservers' reproducibility and agreement for CT interpretation was assessed with overall agreement and Cohen's kappa for dichotomous variables and through Intraclass Correlation Coefficient (ICC) and Information Based Measure of Disagreement (IBMD) for CT severity index. The area under ROC curve (AUC) and 95 % confidence limits were used to assess the predictive power of the CT severity index. Maximum value of Youden's J-index was used to determine the cut-off value with best sensitivity and specificity for the severity index. Two-sided P-values lower than 0.05 were considered statistically significant. All statistical analysis and graphical representations were performed within R Studio, a computing environment for R programming language.

3. Results

Of a total of 164 patients, 93 (56.7 %) were male and 71 (43.3 %) were female. Mean patient age was 64.7 $\pm$ 17.3, ranging from 2 to 96 years. CT examinations were performed on average 10.9 $\pm$ 6.6 days after symptom onset. Respiratory artifacts which degraded image quality were present in 14 examinations (8.4 %). Eleven patients (6.7 %) had a normal chest CT scan. As expected, ground-glass opacities (89.0 %) and consolidations (73.2 %) with multilobar involvement were the predominant imaging findings, while a nodular pattern (3.7 %) and cavitation (1.2 %) were highly uncommon. Most patients (146, 89.0 %) had at least 2 involved lobes, with 114 patients (69.5 %) having involvement of all five pulmonary lobes. Left lower lobe was the most frequently involved lobe (150, 91.5 %), whereas the right middle lobe was the least frequent (129, 78.7 %).

In the two-week follow-up period after the initial CT scan, 130 (79.3 %) patients were either discharged home or admitted to a routine ward (non-ICU), twenty-seven patients (16.4 %) were either deceased or admitted to an intensive care unit (ICU) and 7 patients (4.3 %) were transferred to another institution and follow-up was lost. In the univariate analysis, mean age was significantly higher in the mortality/ICU group (71.1 $\pm$ 12.4 vs. 63.3 $\pm$ 18.2 p = 0.04). Ground-glass opacities and consolidations were the dominant feature in both groups, but distribution pattern of abnormalities was significantly different, being more

Table 1
Epidemiologic and CT imaging features in all patients and in two short-term prognosis groups. Favorable prognosis includes patients either discharged home or admitted to a routine hospital ward (non-ICU). Unfavorable prognosis refers to patients who either died or were admitted to an ICU 14 days after the initial CT scan.

		All patients (n = 164)	Favorable prognosis group (n = 130)	Unfavorable prognosis group (n = 27)	*p value*
Sex, n (%)	Male	93 (56.7 %)	71 (54.6 %)	17 (63.0 %)	0.56
	Female	71 (43.3 %)	59 (45.4 %)	10 (37.0 %)	
Age, mean (SD)		64.7 (17.3)	63.3 (18.2)	**71.1 (12.4)**	**0.036**
Days after onset, mean (SD)		10.9 (6.6)	11.2 (6.7)	8.7 (5.5)	0.097
Origin, n (%)	Outpatient	0 (0.0 %)	0 (0.0 %)	0 (0.0 %)	**<0.001**
	ER	54 (32.9 %)	44 (33.8 %)	4 (14.8 %)	
	Non-ICU ward	100 (61.0 %)	85 (65.4 %)	14 (51.9 %)	
	ICU	10 (6.1 %)	1 (0.8 %)	9 (33.3 %)	
GGO, n (%)		146 (89.0 %)	113 (86.9 %)	26 (96.3 %)	0.29
Consolidation, n (%)		120 (73.2 %)	90 (69.2 %)	24 (88.9 %)	0.065
Nodules, n (%)		6 (3.7 %)	4 (3.1 %)	2 (7.4 %)	0.606
Number of affected lobes, n (%)	0	10 (6.1 %)			
	1	8 (4.9 %)			
	2	5 (3.0 %)			
	3	7 (4.3 %)			
	4	20 (12.2 %)			
	5	114 (69.5 %)			
Number of affected lobes, mean (SD)		4.2 (1.5)	4.1 (1.6)	4.7 (1.0)	0.06
Affected lobes, n (%)	RUL	136 (82.9 %)	104 (80.0 %)	25 (92.6 %)	0.201
	RML	129 (78.7 %)	97 (74.6 %)	25 (92.6 %)	0.074
	RLL	136 (82.9 %)	105 (80.8 %)	24 (88.9 %)	0.467
	LUL	138 (84.2 %)	106 (81.5 %)	25 (92.6 %)	0.262
	LLL	150 (91.5 %)	116 (89.2 %)	27 (100 %)	0.157
Round morphology, n (%)		60 (36.6 %)	**54 (**41.5 %**)**	4 (14.8 %)	**0.016**
Linear opacities, n (%)		81 (49.4 %)	**70 (**53.8 %**)**	7 (25.9 %)	**0.015**
Crazy-paving, n (%)		55 (33.5 %)	41 (31.5 %)	11 (40.7 %)	0.484
Halo sign, n (%)		20 (12.2 %)	17 (13.1 %)	2 (7.4 %)	0.619
Distribution pattern, n (%)	Peripheral	60 (40.0 %)	54 (41.5 %)	4 (14.8 %)	**0.009**
	Central	5 (3.3 %)	4 (3.1 %)	1 (3.7 %)	
	Peripheral + central	85 (56.7 %)	58 (44.6 %)	**22 (**81.5 %**)**	
Cavitation, n (%)		2 (1.2 %)	1 (0.8 %)	1 (3.7 %)	0.769
Lymphadenopathy, n (%)		32 (19.5 %)	22 (16.9 %)	8 (29.6 %)	0.208
Pleural effusion, n (%)		45 (27.4 %)	33 (25.4 %)	10 (37.0 %)	0.318
Underlying lung disease, n (%)		36 (21.9 %)	25 (19.2 %)	9 (33.3 %)	0.173
CT Severity Index, mean (SD)		23.2 (13.1)	20.9 (11.9)	**32.0 (14.4)**	**<0.001**

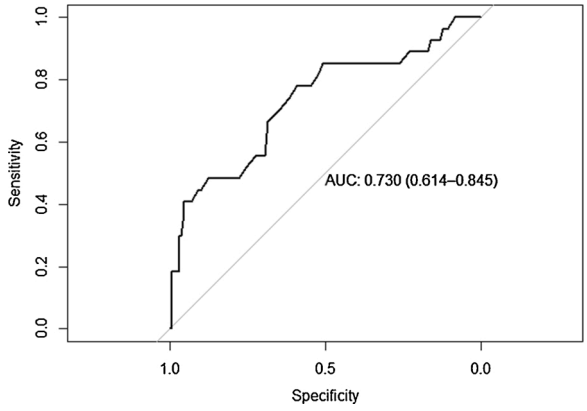

Fig. 1. Receiver Operating Characteristic (ROC) Curve for the CT severity index on unfavorable prognosis at 14 days. AUC, Area Under the Curve.

often diffuse (central + peripheral) in the mortality/ICU group (81.5 % vs. 44.6 % p = 0.01). A purely central distribution was rarely found in all patients (5 of 164, 3.0 %). Linear opacities resembling patterns of organizing pneumonia and opacities that were mostly rounded in shape were more frequently observed in the favorable prognosis group (53.8 % vs. 25.9 %, p = 0.02). Of note, the CT severity index was significantly higher in the mortality/ICU group than in the favorable prognosis group (32.0 ± 14.4 vs. 20.9 ± 11.9 p < 0.001). CT imaging features across the study population are listed in Table 1.

For multivariate analysis and for an initial logistic regression model with stepwise (both directions) selection of variables, the presence of opacities with rounded morphology (OR = 0.2; 95 %CI =]0.04; 0.8[) and the presence of linear opacities consistent with organizing pneumonia (OR = 0.1; 95 %CI =]0.02; 0.39[) were associated with a favorable prognosis at 14 days while the CT severity index (OR = 1.1; 95 %CI =]1.01; 1.13[) and patient origin (non-ICU ward: OR = 3.8; 95 %CI =]0.83; 17.12[; ICU: OR = 53.0; 95 %CI =]2.95; 952.12[) was predictive of a worse outcome. Time of examination after symptom onset was also included in this model, but did not reach a statistically significant result. The Hosmer and Lemeshow goodness of fit (GOF) test had a p-value = 0.293, so we conclude this model is a good fit for the data.

For the assessment of unfavorable prognosis at 14 days by CT severity index we obtained an AUC of 0.73 (Fig. 1). According to the Youden index method, the best cut-off for CT severity index was 24 with a sensitivity of 78 % and a specificity of 59 %.

When considering a CT severity index > 24 as a predictive variable for short-term prognosis instead of CT severity index as a continuous variable, in a logistic regression model, the presence of opacities with rounded morphology and the presence of linear opacities were still predictive of a favorable outcome while a CT severity index > 24 and patient origin remained predictive of a worse outcome. When we excluded patient origin from analysis we obtained a final model in which rounded morphology (OR = 0.2; 95 %CI =]0.04; 0.7[) and linear opacities (OR = 0.1; 95 %CI =]0.03; 0.38[) are protective factors and CT severity index ≥ 24 (OR = 5.6; 95 %CI =]1.55; 19.9[) is a risk factor for being either dead or admitted to an ICU at 14 days. For this model we obtained a p-value of 0.94 for the GOF test and we concluded for the good fit of the model to the data.

Agreement between observers within CT findings, was very high with overall agreements almost perfect and kappa values higher than 0.83. Regarding the CT severity index, ICC was 0.94 (95 %CI = [0.92;

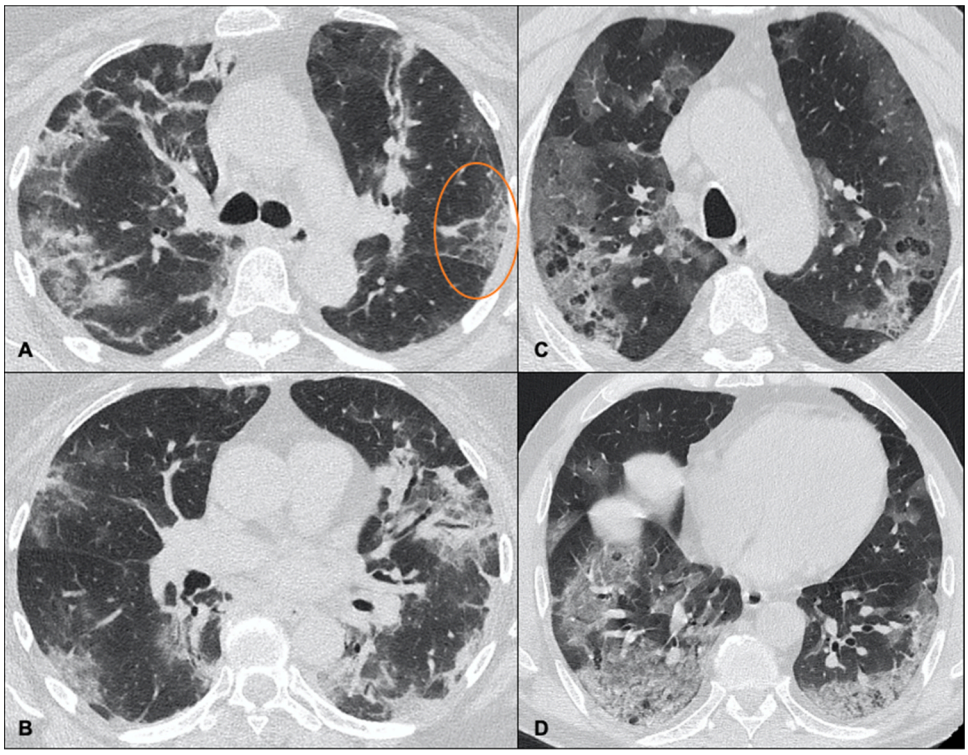

Fig. 2. CT imaging appearance from patients on unfavorable prognosis group. **A** and **B**: CT images from a 65-year-old female patient 9 days after symptom onset showing bilateral, multifocal ground glass and consolidative opacities with both central (peribronchovascular) and peripheral involvement. Some superimposed reticular abnormality (crazy-paving) is noted on left upper lobe (circle). Consensus CT severity index for this patient was 41. **C** and **D**: CT scan from a 72-year-old male patient 4 days after symptom onset depicts extensive bilateral ground-glass opacification with peripheral predominance with some areas of consolidation on both lower lobes. Centrilobular emphysema is also present. CT severity index for this patient was 44.

0.96]) and IBMD was 0.15 (95 %CI = [0.12; 0.18]).

4. Discussion

We conducted this retrospective study to describe the chest CT imaging characteristics in a Portuguese cohort of COVID-19 patients while we also aimed to assess if any of these radiological features was associated with short-term prognosis.

Although CT is considered non-specific for evaluation of COVID-19 pneumonia, our data is consistent with previously reported series [22, 23] in that we found that most patients present with mutifocal, multilobar ground-glass opacities as the predominant imaging pattern. Parenchymal consolidation was also a very common finding. We did not find, however, a clear lower lobe predominant or peripheral predominant distribution of abnormalities, with only 40 % of patients presenting exclusively with a peripheral pattern (although 88 % of patients

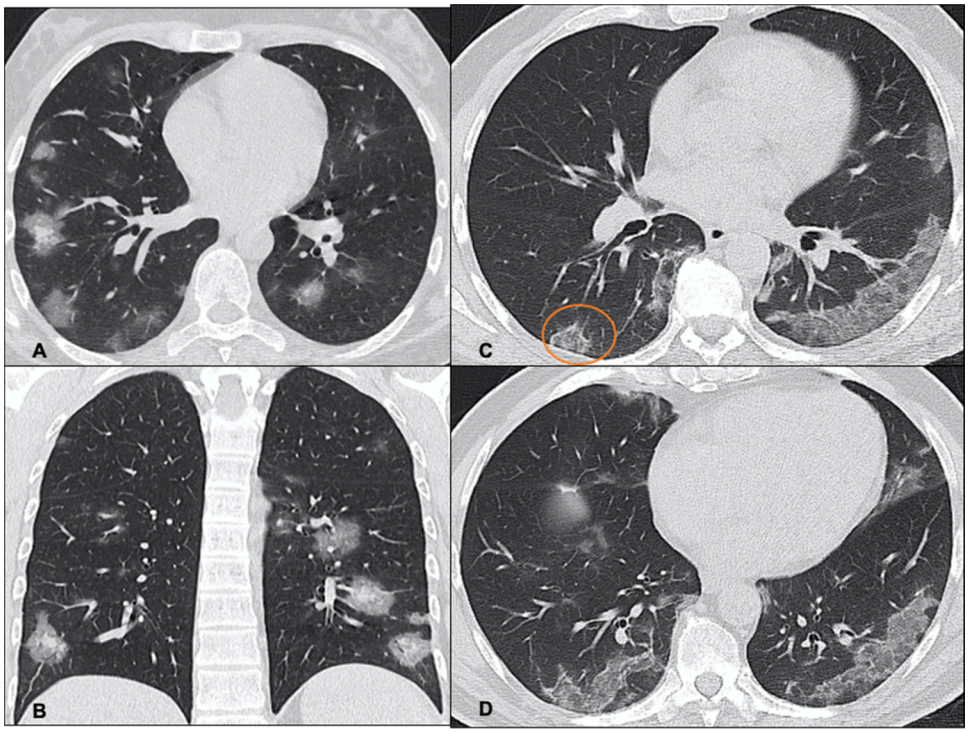

Fig. 3. CT imaging appearance from patients on favorable prognosis group. **A** and **B**: CT images from a 25-year-old female patient 8 days after symptom onset showing bilateral ground-glass opacities with rounded morphology. Note some areas of increased density within ground-glass opacification which could represent either subsegmental vessel enlargement or foci of consolidation (*halo sign*). CT severity index = 20. **C** and **D**: CT scan from a 65-year-old male 12 days after symptom onset. Bilateral peripheral ground-glass opacities are noted. Surrounding some of these opacities we can see a thin line of consolidation (reverse halo sign, circle), suggesting organizing pneumonia.

ultimately had peripheral involvement). Important negatives were, as expected, the presence of cavitation (in fact, our 2 cases with cavitation were assumed to be related to superimposed bacterial infection) and a nodular/micronodular pattern of disease. We also reported a slightly higher prevalence of pleural effusions (27 %), which we postulated that can be related to the relatively higher mean age of our cohort (65 years). We have also found a relatively higher than normal proportion of patients with lymphadenopathy (20 %), yet not as high as described in Rome, Italy [15].

For assessing short-term prognosis, patients were divided into two distinct groups according to their status at 14 days after the initial CT examination: a favorable prognosis group (patients either discharged or admitted to a non-ICU ward) and an unfavorable prognosis group (patients who either died or were admitted to an ICU). When these prognostic groups were compared, we found that older age, pulmonary opacities with diffuse distribution in the axial plane (both peripheral and central) and a higher CT severity index were all associated with a worse outcome (Fig. 2). Consolidations were most commonly found on the unfavorable prognosis group but this difference did not reach statistical significance (88.9 % vs. 69.2 %, $p = 0.06$). We also did not find significant differences in prevalence of a crazy-paving pattern or the halo sign, pleural effusions, lymphadenopathy or underlying lung disease between groups. A diffuse pattern (peripheral + central) could probably be related to more severe patterns of lung damage (e.g. diffuse alveolar damage) and may impact prognosis. An ideal cut-off value for the CT severity index of 24 (sensitivity of 78 % and specificity of 59 %) was found, which is in keeping with the findings recently reported by Yuan and colleagues [24] (albeit with reduced sensitivity and specificity). This data supports the idea that the volume of affected lung may have a key role in clinical severity of SARS-CoV-2 pneumonia [25–27].

On the other hand, the presence of opacities with rounded morphology and findings suggesting organizing pneumonia (band-like opacities, perilobular opacities and reversed halo sign) were associated with favorable outcome (Fig. 3) and this association kept statistically significant even after multivariate analysis and after adjusting for the CT severity index. Organizing pneumonia patterns have been previously associated with stable disease [28] but, to the best of our knowledge, the association between pulmonary opacities with rounded morphology and favorable short-term prognosis has not yet been previously described.

We found a very high interobserver agreement, not only for each isolated imaging finding (kappa values > 0.83 across all variables) but also on applying the CT severity index, despite the considerable different levels of expertise between radiologists. Also, from our personal experience, application of such score was not an extensively time-consuming task. This adds value to this type of visual scoring system, as the lack of information on interobserver agreement was a limitation in the study by Yuan et al. [24].

Our study is not without limitations. First, it is a retrospective study from a single center. The proportion of examinations with considerable respiratory artifacts was not negligible (8%). These artifacts impair image interpretation and can lead to overestimation of ground-glass opacification. Also, we did not incorporate clinical data in the analysis as this was designed to be a radiological study. However, the presence of underlying lung disease (as far as can be ascertained by the radiologist, such as the presence of emphysema, bronchiectasis or imaging findings of lung fibrosis) did not differ between prognostic groups. CT examinations were performed quite late in the course of the disease. This may be explained because during the first weeks of the pandemic, CT was requested only for hospitalized patients who were not responding to supportive treatment. Lastly, we did not specifically evaluate some important CT features known to be associated with COVID-19 pneumonia, (e.g., subsegmental vascular enlargement). These may be targeted in future studies.

5. Conclusion

COVID-19 pneumonia in Porto, Portugal, manifests as multilobar ground-glass opacities and consolidations. Older age and diffuse distribution of abnormalities in the axial plane and are associated with worse short-term prognosis while the presence of linear opacities resembling organizing pneumonia and opacities that are rounded in shape herald a more favorable prognosis. A CT severity index > 24 is a reproducible measure for assessing short-term prognosis in these patients.

Ethical disclosures

All procedures performed in studies involving human participants were in accordance with the ethical standards of the institutional and/or national research committee and with the 1964 Helsinki declaration and its later amendments or comparable ethical standards.

Funding

None.

SD, standard deviation; ICU, intensive care unit; ER, emergency room; GGO, ground glass opacities; RUL, right upper lobe; RML, right middle lobe; RLL, right lower lobe; LUL, left upper lobe; LLL, left lower lobe.

CRediT authorship contribution statement

A. Carvalho: Conceptualization, Methodology, Investigation, Writing - original draft. **R. Cunha:** Conceptualization, Methodology, Investigation, Writing - original draft. **B.A. Lima:** Conceptualization, Methodology, Formal analysis, Writing - original draft. **J.M. Pereira:** Conceptualization, Methodology, Supervision, Writing - review & editing. **A.J. Madureira:** Conceptualization, Methodology, Supervision, Writing - review & editing.

Declaration of Competing Interest

The authors declare that they have no conflicts of interest.

References

[1] N. Zhu, D. Zhang, W. Wang, X. Li, B. Yang, J. Song, et al., A novel coronavirus from patients with pneumonia in China, 2019, N. Engl. J. Med. 382 (8) (2020) 727–733, https://doi.org/10.1056/NEJMoa2001017.
[2] World Health Organization, Weekly Operational Update on COVID-19, World Health Organization, Geneva, 2020 [Available from: https://www.who.int/docs/default-source/coronaviruse/situation-reports/wou-4-september-2020-approved.pdf?sfvrsn=91215c78_4].
[3] Z.J. Cheng, J. Shan, 2019 Novel coronavirus: where we are and what we know, Infection 48 (2) (2020) 155–163, https://doi.org/10.1007/s15010-020-01401-y.
[4] H.A. Rothan, S.N. Byrareddy, The epidemiology and pathogenesis of coronavirus disease (COVID-19) outbreak, J. Autoimmun. (2020), 102433, https://doi.org/10.1016/j.jaut.2020.102433.
[5] A.J. Rodriguez-Morales, J.A. Cardona-Ospina, E. Gutierrez-Ocampo, R. Villamizar-Pena, Y. Holguin-Rivera, J.P. Escalera-Antezana, et al., Clinical, laboratory and imaging features of COVID-19: a systematic review and meta-analysis, Travel Med. Infect. Dis. (2020), 101623, https://doi.org/10.1016/j.tmaid.2020.101623.
[6] DGS relatório de situação COVID-19 [Available from: https://covid19.min-saude.pt/wp-content/uploads/2020/09/186_DGS_boletim_20200904.pdf].
[7] Z. Ye, Y. Zhang, Y. Wang, Z. Huang, B. Song, Chest CT manifestations of new coronavirus disease 2019 (COVID-19): a pictorial review, Eur. Radiol. 30 (2020) 4381–4389, https://doi.org/10.1007/s00330-020-06801-0.
[8] Z. Cheng, Y. Lu, Q. Cao, L. Qin, Z. Pan, F. Yan, et al., Clinical features and chest CT manifestations of coronavirus disease 2019 (COVID-19) in a single-center study in Shanghai, China, AJR Am. J. Roentgenol. (2020) 1–6, https://doi.org/10.2214/AJR.20.22959.
[9] R. Han, L. Huang, H. Jiang, J. Dong, H. Peng, D. Zhang, Early Clinical and CT Manifestations of Coronavirus Disease 2019 (COVID-19) Pneumonia, AJR Am. J. Roentgenol. (2020) 1–6, https://doi.org/10.2214/AJR.20.22961.
[10] Y. Li, L. Xia, Coronavirus Disease 2019 (COVID-19): Role of Chest CT in Diagnosis and Management, AJR Am. J. Roentgenol. (2020) 1–7, https://doi.org/10.2214/AJR.20.22954.

[11] S. Zhou, Y. Wang, T. Zhu, L. Xia, CT features of coronavirus disease 2019 (COVID-19) pneumonia in 62 patients in Wuhan, China, AJR Am. J. Roentgenol. (2020) 1–8, https://doi.org/10.2214/AJR.20.22975.
[12] X. Zhao, B. Liu, Y. Yu, X. Wang, Y. Du, J. Gu, et al., The characteristics and clinical value of chest CT images of novel coronavirus pneumonia, Clin. Radiol. 75 (5) (2020) 335–340, https://doi.org/10.1016/j.crad.2020.03.002.
[13] Z. Zhou, D. Guo, C. Li, Z. Fang, L. Chen, R. Yang, et al., Coronavirus disease 2019: initial chest CT findings, Eur. Radiol. 30 (2020) 4398–4406, https://doi.org/10.1007/s00330-020-06816-7.
[14] H. Shi, X. Han, N. Jiang, Y. Cao, O. Alwalid, J. Gu, et al., Radiological findings from 81 patients with COVID-19 pneumonia in Wuhan, China: a descriptive study, Lancet Infect. Dis. 20 (4) (2020) 425–434, https://doi.org/10.1016/S1473-3099(20)30086-4.
[15] D. Caruso, M. Zerunian, M. Polici, F. Pucciarelli, T. Polidori, C. Rucci, et al., Chest CT features of COVID-19 in Rome, Italy, Radiology (2020), 201237, https://doi.org/10.1148/radiol.2020201237.
[16] F. Pan, T. Ye, P. Sun, S. Gui, B. Liang, L. Li, et al., Time Course of Lung Changes On Chest CT During Recovery From 2019 Novel Coronavirus (COVID-19) Pneumonia, Radiology (2020), 200370, https://doi.org/10.1148/radiol.2020200370.
[17] F. Song, N. Shi, F. Shan, Z. Zhang, J. Shen, H. Lu, et al., Emerging 2019 novel coronavirus (2019-nCoV) pneumonia, Radiology 295 (1) (2020) 210–217, https://doi.org/10.1148/radiol.2020200274.
[18] H.Y.F. Wong, H.Y.S. Lam, A.H. Fong, S.T. Leung, T.W. Chin, C.S.Y. Lo, et al., Frequency and distribution of chest radiographic findings in COVID-19 positive patients, Radiology (2019), 201160, https://doi.org/10.1148/radiol.2020201160.
[19] X. Xie, Z. Zhong, W. Zhao, C. Zheng, F. Wang, J. Liu, Chest CT for typical 2019-nCoV pneumonia: relationship to negative RT-PCR testing, Radiology (2020), 200343, https://doi.org/10.1148/radiol.2020200343.
[20] D.M. Hansell, A.A. Bankier, H. MacMahon, T.C. McLoud, N.L. Muller, J. Remy, Fleischner Society: glossary of terms for thoracic imaging, Radiology 246 (3) (2008) 697–722, https://doi.org/10.1148/radiol.2462070712.
[21] F. Feng, Y. Jiang, M. Yuan, J. Shen, H. Yin, D. Geng, et al., Association of radiologic findings with mortality in patients with avian influenza H7N9 pneumonia, PLoS One 9 (4) (2014), e93885, https://doi.org/10.1371/journal.pone.0093885.
[22] S. Salehi, A. Abedi, S. Balakrishnan, A. Gholamrezanezhad, Coronavirus Disease 2019 (COVID-19): A Systematic Review of Imaging Findings in 919 Patients, AJR Am. J. Roentgenol. (2020) 1–7, https://doi.org/10.2214/AJR.20.23034.
[23] S. Manna, J. Wruble, S.Z. Maron, D. Toussie, N. Voutsinas, M. Finkelstein, et al., COVID-19: a multimodality review of radiologic techniques, clinical utility, and imaging features, Radiol. Cardiothoracic Imaging 2 (3) (2020), https://doi.org/10.1148/ryct.2020200210.
[24] M. Yuan, W. Yin, Z. Tao, W. Tan, Y. Hu, Association of radiologic findings with mortality of patients infected with 2019 novel coronavirus in Wuhan, China, PLoS One 15 (3) (2020), e0230548, https://doi.org/10.1371/journal.pone.0230548.
[25] R. Zhang, H. Ouyang, L. Fu, S. Wang, J. Han, K. Huang, et al., CT features of SARS-CoV-2 pneumonia according to clinical presentation: a retrospective analysis of 120 consecutive patients from Wuhan city, Eur. Radiol. 30 (2020) 4417–4426, https://doi.org/10.1007/s00330-020-06854-1.
[26] D. Colombi, F.C. Bodini, M. Petrini, G. Maffi, N. Morelli, G. Milanese, et al., Well-aerated lung on admitting chest CT to predict adverse outcome in COVID-19 pneumonia, Radiology (2020), 201433, https://doi.org/10.1148/radiol.2020201433.
[27] M. Yu, D. Xu, L. Lan, M. Tu, R. Liao, S. Cai, et al., Thin-section Chest CT Imaging of Coronavirus Disease 2019 Pneumonia: Comparison Between Patients with Mild and Severe Disease, Radiol. Cardiothoracic Imaging 2 (2) (2020), https://doi.org/10.1148/ryct.2020200126.
[28] S.M.H. Tabatabaei, H. Talari, F. Moghaddas, H. Rajebi, Computed Tomographic Features and Short-term Prognosis of Coronavirus Disease 2019 (COVID-19) Pneumonia: A Single-Center Study from Kashan, Iran, Radiol. Cardiothoracic Imaging 2 (2) (2020), https://doi.org/10.1148/ryct.2020200130.